SEMI-OBJECTIVE DETERMINATION OF LITHOLOGIC END-MEMBERS IN A GEOLOGIC ENVIRONMENT (SPECTRAL MIXTURE ANALYSIS) Stefanie Tompkins, John F. Mustard, Carlé M. Pieters, Donald W. Forsyth, Dept. Geol. Sci., Box 1846, Brown University, Providence, RI 02912

Introduction: Spectral mixture analysis (SMA) has been shown to be a powerful tool for the analysis and geological interpretation of planetary multispectral images (1-3). The underlying assumption of SMA is that each pixel on the surface is a physical mixture of several components, and the spectrum of the mixture a linear combination of the end-member reflectance spectra. The spectral variability of a scene is thus modeled as a linear combination of a small number of spectral end-members (which are usually expected to be end-members on the ground, as well). The strength of this approach lies in three major areas: it is a physically based model that transforms reflectance values to physical variables, it provides a means to detect and represent components that occur at a sub-pixel level, and it provides quantitative results that can in turn be incorporated into models of surface processes within the image scene. However, issues remain concerning the selection of spectral end-members and the interpretation of fraction images that must be resolved. SMA results must be repeatable, and the fraction images must describe realistic physical variables of components in the scene. If not, SMA becomes little more than an image classification technique.

End-member Selection: The repeatability and physical interpretation of end-member fraction images depends on the accuracy of the spectral end-members that are used to model the data. End-members are usually selected through an educated trial-and-error process: the analyst selects those areas in an image that are expected to represent end-members, finds the fraction images of those end-members, and uses the error of the model fit to improve the initial end-member selection. The process is highly subjective, often based on *a priori* knowledge of the geologic setting, but may be preferable to the extreme alternative: selection of end-member spectra by purely statistical methods (e.g., principal components, or factor analysis). While the latter method is objective, and is repeatable for a given image, the end-member spectra may not be realistic in a physical sense. An alternative approach is to combine the statistical and subjective methods (as described below, and in detail in 4) to find end-members that are believed to model the mixing of surface materials, and still satisfy statistical requirements imposed by the variance of the spectral data at the sub-pixel level.

Modified SMA (MSMA): The fundamental equations of spectral mixture analysis are:

$$\sum_b R_b = \sum_b \sum_i r_{ib} f_i + \sum_b E_b \quad \text{and} \quad \sum_i f_i = 1.0$$

where f_i is the fractional abundance of end-member i in a given pixel, R_b is the total reflectance of the pixel in band b, r_{ib} is the reflectance of end-member i in band b, and E_b is the residual error in band b. In the classic SMA, the end-members are selected first, and their fractional distribution found within the image scene. In the modified method, both end-member spectra and fractional abundance are treated as unknowns. In order to solve this type of non-linear equation, a starting model is provided, and a solution is found through iteration using a damped least squares stochastic inversion (5). The evolution of end-member spectra and fractions from the starting model to the solution is governed by a number of constraints imposed on the calculations, that are essentially quantitative descriptions of *a priori* knowledge. These constraints are applied in the form of additional equations, the starting model itself, and covariance matrices for both the data (pixel spectra) and the model parameters (end-member spectra and fractions). Exact matches to the derived end-member spectra may not necessarily be found within the original data set. However, these "virtual end-members" appear to represent mixing end-members that are more spectrally pure, and which may be more closely matched to library or reference end-members.

Lunar Crater Example: The modified mixing model has been applied to 8-band CCD images of the lunar crater Bullialdus. In Figure 1, the starting model spectra are shown in solid lines, and the virtual end-members derived by MSMA in dashed lines. The kinds of constraints used to derive this solution should help to clarify the MSMA approach. First, since the geology of Bullialdus had been previously studied (6, 7), the starting model end-members were selected from within the image where distinct units were expected to occur. Thus spectra from the central peaks, floor, walls and immediate ejecta of the crater were selected to be end-members for the starting model. They were then allowed to vary by different amounts, depending on *a priori* information. The central peaks, for example, are known to be distinct from the rest of the crater (6, 7), and to mix very little with other crater materials. Therefore the starting model spectrum for the peaks was assumed to be well known, and allowed to vary less than the other three end-members. The starting model fractional abundances were set at 0.5, and all were allowed to deviate ±0.5 (i.e., the fractions were allowed to vary between 0 and 1). Variances were applied to the data as well, in the data covariance matrix. Standard deviations of 10x10 pixel areas within the image were used to determine the variance of each channel. The variance was allowed to increase for those channels where problems with image registration were known to add noise. The final solution was reached when a predetermined error threshold was passed. In this example, the virtual end-members better model the image data in that the rms error is lower, and the fraction images are spatially coherent with no negative or superpositive values. However, several questions remain. The most important is whether the virtual end-members represent real materials that exist at sub-pixel levels within the image. This becomes a critical issue if the end-members are not as well known ahead of time as they were for this example. In such a case, one or more end-members could be a straight line in the starting model, and assigned a high variance. The MSMA would then derive virtual end-member spectra (as has been demonstrated for a terrestrial data set, 4), but it remains to be proven that the virtual end-members are truly part of the image scene. Another question concerns the possible uses of constraints. In this example, the different Bullialdus channels were weighted unequally to account for noise in different channels. However, they could also be weighted unequally to examine a specific scientific question. For lunar spectra, this type of weighting could be used to subdue the effects of the 0.40-0.56 μm slope (strongly linked to maturity), and to emphasize the effects of channels in the 1-μm region (where absorptions are linked to composition as well as maturity) when determining spectral end-members. Other constraints may be added in the form of additional equations to the model. In the lunar case, end-member spectra could be required to have a positive slope between 0.40 and 0.70 μm. A broader application would be to constrain the interaction of specific end-members that are known always or never to be located together on the ground.

Simulated Crater Example: In order to answer these questions, and to test more thoroughly the applications of both the traditional SMA and our modified SMA, a simulated lunar crater image is currently being developed. For this simulated crater, the abundances of end-members (representing immature central peaks, wall, a mare component) are predetermined based on simple cratering models, and their spectra mixed together in either a linear or non-linear (8) fashion. A topographic model for the crater is included in the simulation, to explicitly incorporate shade as a variable. The spatial resolution of the image is then degraded, to represent the type of data that is generally available for planetary study, and to ensure that the end-members do not make up 100% of any single pixel. The virtual end-members that are derived for the image can then be compared to the "true" end-members that created the simulation. The first test is focused wholly on the behavior of the MSMA itself: to determine whether or not the true end-members can be derived from this simulated image, and what constraints are required to do so. Both random and non-random noise (such as arise from registration or calibration errors) may be added to the image as well, in order to determine the adjustments that must be made to the constraints under these conditions. Ideally, similar constraints may be applied to a real image, and any inconsistencies between the artificial and true image results can be used to further modify the artificial image and find new constraints.

However, it is simplistic to expect tests such as those described here to directly affect the geologic interpretation of the image data. The model crater is an extremely simple representation of what is obviously a complex geological feature. Therefore, it is anticipated that as research progresses, the simulated image will be further developed in a geological sense to reflect more accurately those lunar processes that are known to occur, such as space weathering, complex mixing on the crater floor, etc. As the development of the simulated image occurs, the use of constraints to examine specific science questions can be further explored as well. Ultimately, the results of SMA and MSMA applied to a simulated image can be directly compared to those obtained from real craters such as Bullialdus or from lunar basins, in order to guide the geologic interpretation of the mixing model solutions.

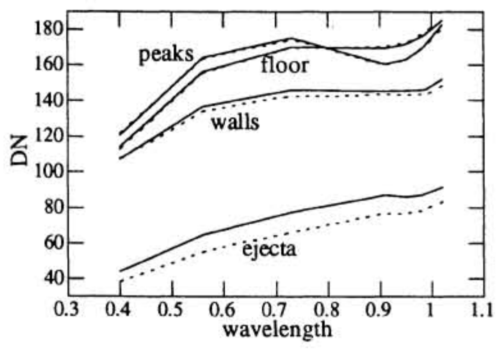

Figure 1: MSMA End-member Spectra. Solid lines represent starting model spectra. Dashed lines are model-derived virtual end-members.

Acknowledgements: This research was supported in part by NASA grant NAGW-28 (CMP) and JPL Contract 959-228 (JFM).

References: (1) Adams et al. (1986) *J. Geophys. Res., 91*: 8098-8112. (2) Head et al. (1993) *J. Geophys. Res., 98*, 17,149-17,181. (3) Adams et al.(1993) in *Remote Geochemical Analysis: Elemental and Mineralogical Composition*, Pieters and Englert, eds., 145-166. (4) Tompkins et al. (1993) *JPL Pub. 93-26, v. 1*, 177-180. (5) Tarantola and Valette (1982) *Rev. Geophys. Space. Phys.*, 20: 219-232. (6) Pieters, (1991) *Geophys. Res. Let.*, 18: 2129-2132. (7) Tompkins et al. (1993) *LPSC 24*, 1433-1434. (8) Hapke (1981) *J. Geophys. Res., 86*, 3039-3054.